Supporting Information

Kong et al. 10.1073/pnas.1202924109

SI Materials and Methods

Cells, Antibodies, Viruses, and Peptides. Huh-7 (1) and 293T cells were grown in DMEM supplemented with 10% FCS (Invitrogen). The human mAbs AR2A and AR3A (2) and mouse mAb A4 (3) have been described elsewhere. Recombinant mAb HCV1 (4) was produced as below. The methods for generating hepatitis C virus pseudotype virus particles (HCVpp) have been previously described (2, 5, 6). The R12-mer and 15-mer peptides were synthesized by GenScript (>95% purity). The 18-mer overlapping peptide library of the H77 isolate was provided by the National Institutes of Health AIDS Research and Reference Reagent Program.

Expression of Recombinant mAb HCV1. The variable domains of heavy and light chains of mAb HCV1 (4) were synthesized (GenScript) and cloned into the pIgG1 vector (2) for expression as a full-length human IgG1. The mAb was produced in CHO-K1 cells stably transfected with the expression vector and purified over a protein A-affinity column (GE Healthcare). To express Fab fragments for crystallization, the hinge, C_H2, and C_H3 sequences of mAb HCV1 cloned into the pIgG1 expression vector were removed. The Fab fragment was produced by transient transfection of FreeStyle 293-F cells and purified using a rabbit anti-human Fab antibody affinity column.

ELISA. To determine whether the antibodies recognized native, reduced, or mutant E2, the E1E2 antigens were captured onto ELISA wells that were precoated with *Galanthus nivalis* lectin (5 μg/mL; Sigma) (folded protein) or unfolded with 0.1% SDS, 50 mM DTT, and incubated at 100 °C for 5 min before capture onto ELISA wells (unfolded protein). E1E2 and mutant antigens were prepared from cell lysates of 293T cells transfected with H77 E1E2-expression plasmid (7). Nonfat milk (4%; BioRad) in PBS and 0.05% Tween 20 was used as a blocker in assays using lectin-captured antigens. The ELISA plates were washed after 1-h incubation, and binding of antibodies was detected by peroxidase (HRP)-conjugated goat anti-human IgG Fc or anti-mouse IgG secondary antibody (1:2,000) (Pierce) and 3,3′,5,5′-tetramethylbenzidine (TMB) substrate (Pierce).

To study the peptide specificity of mAb HCV1, serially diluted mAb was added to the microwells coated with the peptides. The 15-mer and 18-mer were first dissolved at 1 mg/mL in 100% DMSO before being diluted in PBS for coating, whereas the R12-mer was dissolved directly in PBS at 1 mg/mL After 1-h incubation the plates were washed, and bound antibodies were detected with HRP-conjugated goat anti-human $F(ab')_2$ antibody (Pierce) (1:2,000) and TMB substrate.

To study the ability of peptides in inhibiting mAb HCV1 binding to E1E2, the peptides and mAb were mixed at the specified ratio and incubated for 30 min before adding to ELISA microwells coated with lectin-captured E1E2. After 1-h incubation the plates were washed, and bound antibody was detected with secondary antibody and chromatogenic substrate as above.

To study the apparent affinity of the mAb, serially diluted mAb (twofold dilution from 10 μg/mL) were added to lectin-captured E1E2 antigens for 1 h. The binding of human mAbs was detected by HRP-conjugated goat anti-human IgG $F(ab')_2$ antibody as above. Noninfected/nontransfected cell lysates were used as negative controls to determine background for the mAb. Apparent affinity was defined by the molar concentration of mAbs that produced half of the maximal specific binding in the fitted EC_{50} titration curves using GraphPad Prism software.

Crystallization and Data Collection. The purified Fab was concentrated to 10 mg/mL in 20 mM Tris·HCl and 140 mM NaCl (pH 7) buffer and allowed to form a complex with the R12-mer at a 1:10 molar ratio (protein:peptide) overnight at 4 °C. The HCV1 Fab/E2 peptide ligand complex was screened for crystallization using the International AIDS Vaccine Initiative (IAVI)-Joint Center for Structural Genomics (JCSG)-The Scripps Research Institute (TSRI) CrystalMation robot (Rigaku) that tested 384 crystallization conditions representing the JCSG core crystallization suite at 4° and 20 °C with drops of 100 nL protein mixed with 100 nL well solution (8). Multiple crystals were obtained in several PEG-containing conditions. Crystals were cryoprotected by a brief immersion in 70% well buffer and 30% glycerol, followed by immediate flash-cooling in liquid nitrogen. Two datasets were collected for two crystals at the Advanced Photon Source (APS) beamline 23ID-D. The C2 form crystal was grown in 25% PEG 4000, 0.2 M ammonium sulfate, and 0.1 M sodium acetate (pH 4.6), whereas the $P2_1$ form crystal was grown in 40 mM potassium dihydrogen phosphate, 20% glycerol, and 16% PEG 8000. Both crystals diffracted to a resolution of 1.8 Å, with an overall R_{sym} of 8% and 11% to above 98% completeness (Table S1). Data were processed and scaled with HKL-2000 (9). The space groups are $P2_1$ and C2 with unit cell parameters a = 44.0 Å, b = 75.3 Å, c = 60.8 Å, β= 91.5° and a = 141.1 Å, b = 63.1 Å, c = 69.3 Å, β= 95.7°, respectively.

Structure Determination and Refinement. The structure was determined by the molecular replacement method using Phaser, with data to 1.8-Å resolution using an unrelated anti-CD20 Fab structure (Protein Data Bank ID code 3GIZ) as an initial model. Model building was carried out using Coot-0.6.2 (10), and refinement was implemented with the PHENIX program (11). Final R_{cryst} and R_{free} values are 18.8% and 22.1%, respectively, for the C2 crystal form and 17.1% and 21.4% for the $P2_1$ crystal form. Electron density for the peptide epitope was clear in both crystal forms (Fig. S7). Buried molecular surface areas were analyzed with MS (12) using a 1.7-Å probe radius and standard van der Waals radii, and van der Waals contacts and hydrogen bonds were evaluated with Contacsym (13, 14) and HBPLUS (15). Surface potential and electrostatics were calculated using the adaptive Poisson-Boltzmann solver (16), and all structural visualizations were generated with PyMOL (PyMOL Molecular Graphics System, version 1.2r3pre; Schrödinger, LLC.). For the Fab, the residues were renumbered according to the Kabat scheme (17).

E2 Mutagenesis. Some of the alanine scanning mutants of the E2 CD81-binding site used in this study were generated previously by Owsianka et al. (18). The other mutants were generated using the same E1E2 expression vector as the template (clone H77C) (19). The mutants were generated using the QuikChange Lightning Site-Directed Mutagenesis Kit (Stratagene) and PCR primers encoding the specific mutations (Integrated DNA Technologies). The mutated sequences were confirmed by DNA sequencing.

HCV Neutralization Assays. Neutralization assays were performed in DMEM supplemented with 10% FCS (Invitrogen). HCVpp was generated by cotransfection of 293T cells with pNL4-3.lucR-E- (20, 21) and the corresponding expression plasmids encoding the E1E2 genes at 4:1 ratio by polyethylenimine (22). Virus infectivity was detected using the firefly luciferase assay system (Promega), and percent neutralization was calculated as residual virus infectivity at the indicated antibody concentrations divided by infectivity without antibody after background subtraction.

Background infectivity of the pseudotype virus was determined using cells transfected with pNL4-3.lucR-E- only, and VSVpp was a control for nonspecific activity. In the neutralization assay, the virus was incubated with the diluted antibodies for 1 h at 37 °C before being added to Huh-7 cell monolayers and incubated for another 6 h. To ensure the quality of data for determining virus neutralization, only the data generated with HCVpp with an S/N ratio (signal-to-noise ratio of virus infectivity by HCVpp vs. pseudotype virus generated without E1E2) >10 were considered reliable.

1. Zhong J, et al. (2005) Robust hepatitis C virus infection in vitro. *Proc Natl Acad Sci USA* 102:9294–9299.
2. Law M, et al. (2008) Broadly neutralizing antibodies protect against hepatitis C virus quasispecies challenge. *Nat Med* 14:25–27.
3. Dubuisson J, et al. (1994) Formation and intracellular localization of hepatitis C virus envelope glycoprotein complexes expressed by recombinant vaccinia and Sindbis viruses. *J Virol* 68:6147–6160.
4. Broering TJ, et al. (2009) Identification and characterization of broadly neutralizing human monoclonal antibodies directed against the E2 envelope glycoprotein of hepatitis C virus. *J Virol* 83:12473–12482.
5. Bartosch B, Dubuisson J, Cosset FL (2003) Infectious hepatitis C virus pseudo-particles containing functional E1-E2 envelope protein complexes. *J Exp Med* 197:633–642.
6. Hsu M, et al. (2003) Hepatitis C virus glycoproteins mediate pH-dependent cell entry of pseudotyped retroviral particles. *Proc Natl Acad Sci USA* 100:7271–7276.
7. McKeating JA, et al. (2004) Diverse hepatitis C virus glycoproteins mediate viral infection in a CD81-dependent manner. *J Virol* 78:8496–8505.
8. Newman J, et al. (2005) Towards rationalization of crystallization screening for small- to medium-sized academic laboratories: The PACT/JCSG+ strategy. *Acta Crystallogr D Biol Crystallogr* 61:1426–1431.
9. Otinawski Z, Minor W (1997) Processing of X-ray diffraction and data collected in oscillation mode. *Methods Enzymol* 276:307–326.
10. Emsley P, Lohkamp B, Scott WG, Cowtan K (2010) Features and development of Coot. *Acta Crystallogr D Biol Crystallogr* 66:486–501.
11. Adams PD, et al. (2010) PHENIX: A comprehensive Python-based system for macromolecular structure solution. *Acta Crystallogr D Biol Crystallogr* 66:213–221.
12. Connolly ML (1993) The molecular surface package. *J Mol Graph* 11:139–141.
13. Sheriff S, Hendrickson WA, Smith JL (1987) Structure of myohemerythrin in the azidomet state at 1.7/1.3 A resolution. *J Mol Biol* 197:273–296.
14. Sheriff S, et al. (1987) Three-dimensional structure of an antibody-antigen complex. *Proc Natl Acad Sci USA* 84:8075–8079.
15. McDonald IK, Thornton JM (1994) Satisfying hydrogen bonding potential in proteins. *J Mol Biol* 238:777–793.
16. Baker NA, Sept D, Joseph S, Holst MJ, McCammon JA (2001) Electrostatics of nanosystems: Application to microtubules and the ribosome. *Proc Natl Acad Sci USA* 98:10037–10041.
17. Martin AC (1996) Accessing the Kabat antibody sequence database by computer. *Proteins* 25:130–133.
18. Owsianka AM, et al. (2006) Identification of conserved residues in the E2 envelope glycoprotein of the hepatitis C virus that are critical for CD81 binding. *J Virol* 80: 8695–8704.
19. Yanagi M, Purcell RH, Emerson SU, Bukh J (1997) Transcripts from a single full-length cDNA clone of hepatitis C virus are infectious when directly transfected into the liver of a chimpanzee. *Proc Natl Acad Sci USA* 94:8738–8743.
20. Connor RI, Chen BK, Choe S, Landau NR (1995) Vpr is required for efficient replication of human immunodeficiency virus type-1 in mononuclear phagocytes. *Virology* 206: 935–944.
21. He J, et al. (1995) Human immunodeficiency virus type 1 viral protein R (Vpr) arrests cells in the G2 phase of the cell cycle by inhibiting p34cdc2 activity. *J Virol* 69: 6705–6711.
22. Boussif O, et al. (1995) A versatile vector for gene and oligonucleotide transfer into cells in culture and in vivo: polyethylenimine. *Proc Natl Acad Sci USA* 92: 7297–7301.

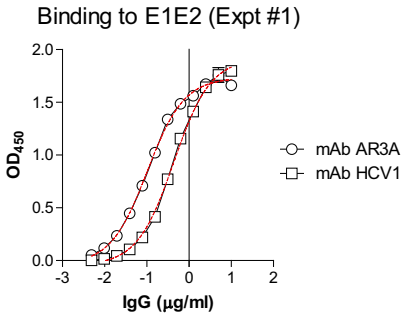

Goodness of Fit		AR3A	HCV1
	R^2	1.00	1.00
EC_{50}	µg/ml	0.10	0.44
	nM	0.69	2.92

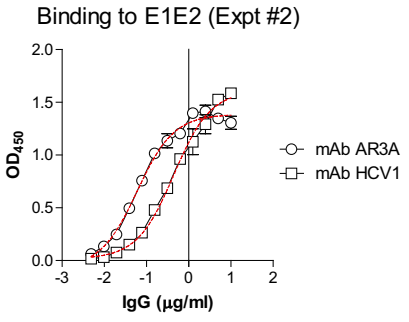

Goodness of Fit		AR3A	HCV1
	R^2	0.99	0.99
EC_{50}	µg/ml	0.06	0.45
	nM	0.40	2.97

		AR3A	HCV1
Mean	nM	0.54	2.95
s.d.		0.20	0.03

Fig. S1. Apparent affinity of mAb HCV1 binding to E1E2 of the prototypic H77 isolate. The mean apparent affinity of mAb and E1E2 determined by ELISA is 3.0 nM. The affinity of mAb HCV1 binding to bacterially expressed thioredoxin fusion protein containing E2 residues 412–423 (Trx-$E2_{412–423}$-His) was determined previously to be 3.8 nM by surface plasmon resonance (4).

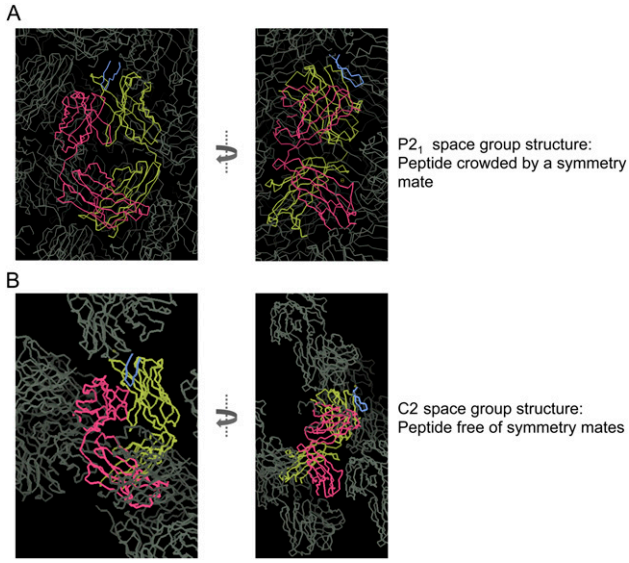

Fig. S2. Crystal packing of the Fab–peptide complex structures. (*A*) Symmetry mates around the Fab–peptide structure in the $P2_1$ form crystal. A symmetry mate is packed close to the binding site. (*B*) Fab–peptide structure in the C2 form is shown with symmetry mates. Here the peptide binding region is free of crystal contacts. Because the peptide is oriented nearly equivalently in the two structures, the binding is unlikely to be affected by crystal packing. Here only the C_α backbone ribbon is shown. The Fab chains and peptide are colored pink, yellow, and blue, whereas the symmetry mates are in gray.

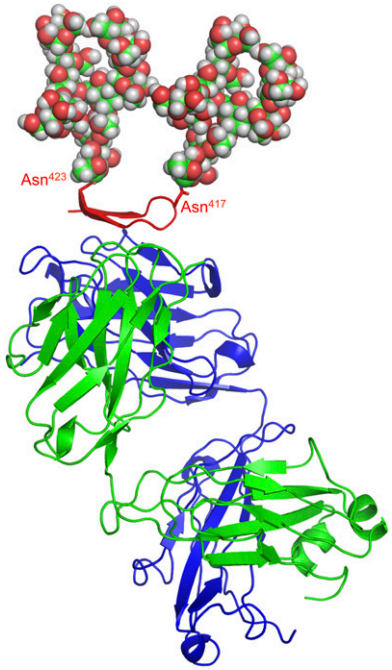

Fig. S3. Modeling of *N*-glycans on the peptide epitope. Two *N*-linked glycosylation sequons on the peptide epitope seem to be functionally important in the virus (1, 2). Here, oligomannose glycans were modeled onto these sites using GlyProt (3). The asparagines in the crystal structure point away from the mAb binding surfaces and orient the glycans away from the Fab.

1. Goffard A, et al. (2005) Role of N-linked glycans in the functions of hepatitis C virus envelope glycoproteins. *J Virol* 79:8400–8409.
2. Helle F, et al. (2010) Role of N-linked glycans in the functions of hepatitis C virus envelope proteins incorporated into infectious virions. *J Virol* 84:11905–11915.
3. Bohne-Lang A, von der Lieth CW (2005) GlyProt: In silico glycosylation of proteins. *Nucleic Acids Res* 33(Web Server issue):W214–W219.

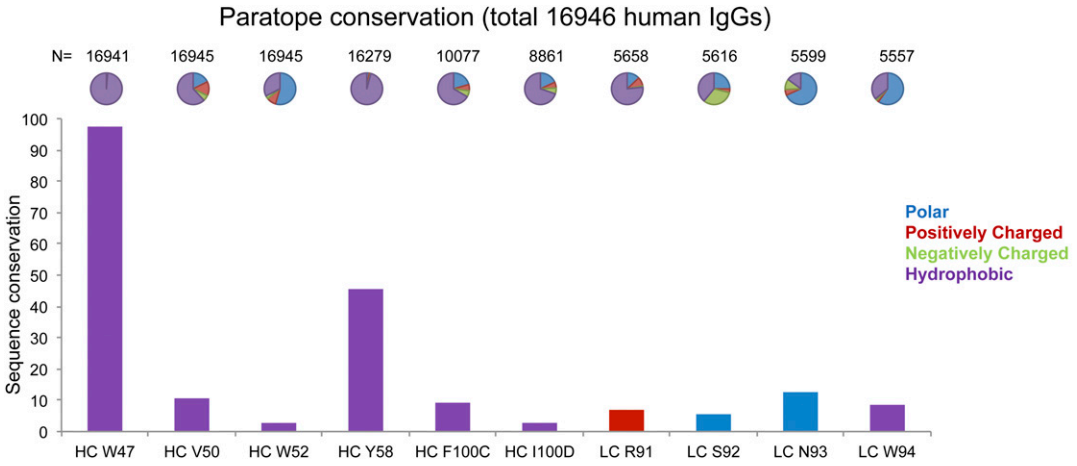

Fig. S4. Paratope conservation of mAb HCV1. The sequence variability of the contacting residues on the mAb across all known unique human IgGs was found using the antibody database developed by Andrew Martin (17). Here we plotted the distribution according to their chemical type using pie charts on top of the overall sequence conservation at those contacting residues that are <4 Å from Trp^{420} and Leu^{413} of the epitope. The residues are labeled X Y#, where X is either heavy chain (HC) or light chain (LC) and Y is a single-letter abbreviation for the amino acid. The # is the sequence number of the residue using the Kabat numbering scheme. As noted in the text, there is high sequence conservation for heavy chain Trp^{47} and heavy chain Tyr^{58} and high chemical-type conservation for the rest of the residues, except for light chain Arg^{91}.

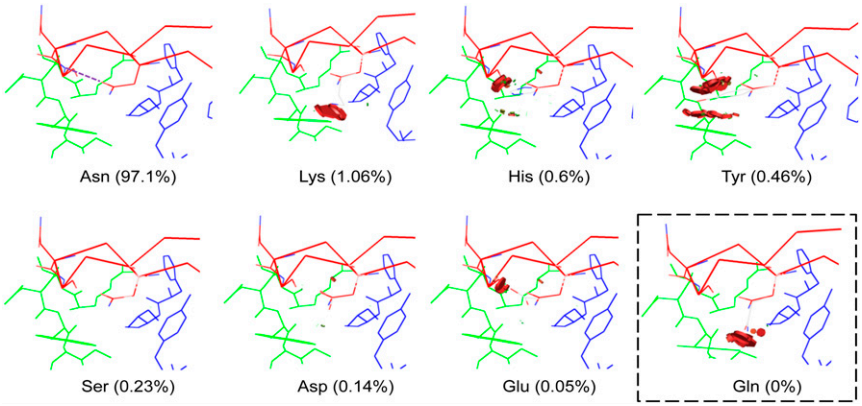

Fig. S5. Potential escape mutations of Asn^{415} on HCV E2. Although predominantly asparagine at position 415 in HCV, mutations at position 415 are found in the natural population (frequency shown in parenthesis), and some may contribute to neutralization escape. A steric clash analysis of allowed side-chain rotamers at position 415 is shown. As in Fig. 2, the peptide is red, light chain is green, and heavy chain is blue. Packing clashes are displayed as red volumes. Only asparagine and aspartic acid at that position can form a stabilizing hydrogen bond to the HCV peptide itself, which is shown as a purple dotted line at *Upper Left*. In addition, serine can be placed without steric clash. However, all other substitutions would result in a clash. Glutamine (boxed) is also analyzed because of its similarity to asparagine, although this mutation has not been found in the National Institute of Allergy and Infectious Diseases Virus Pathogen Database and Analysis Resource (ViPR) database. Shown are the side-chain rotamers with minimal clash.

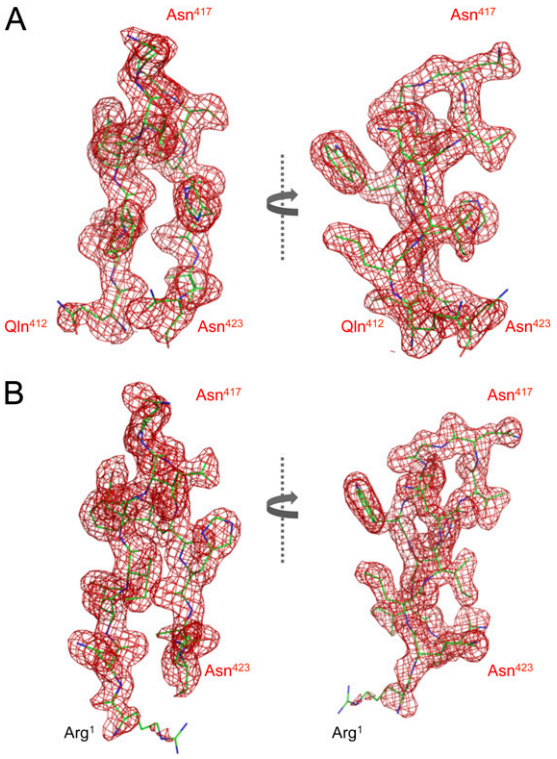

Fig. S6. Electron density of peptide structures. The mFo-DFc maps of the peptide epitope for the C2 (*A*) and $P2_1$ (*B*) crystals are shown at a σ cutoff of 1.0. The peptides are well defined, and we can unambiguously assign the β-turn type and the interactions with the mAb.

Table S1. Data collection and refinement statistics

Data collection	HCV1 Fab-E2 peptide complex C2 form	HCV1 Fab-E2 peptide complex $P2_1$ form
Beamline	APS 23ID-D	APS 23ID-D
Wavelength (Å)	1.033	1.033
Space group	C2	$P2_1$
Unit cell parameters	a = 141.10 b = 63.07 c = 69.30 Å α = γ = 90.0° β = 95.70°	a = 44.04 b = 75.30 c = 60.80 Å α = γ = 90.0° β = 91.53°
Resolution (Å)	28.77–1.80 (1.86–1.80)*	44.04–1.81 (1.84–1.81)*
Observations	207,190	129,576
Unique reflections	55,279 (5,554)*	36,325 (1,809)*
Redundancy	3.7 (3.7)*	3.6 (3.5)*
Completeness (%)	98.9 (100.0)*	99.8 (99.5)*
$<I/\sigma_I>$	13.4 (3.0)*	9.8 (3.0)*
R_{sym} †	0.08 (0.53)*	0.11 (0.62)*
Refinement statistics		
Resolution (Å)	28.77–1.80	44.04–1.81
Reflections (work)	52,268	36,301
Reflections (test)	2,809	1,813
R_{cryst}(%)‡	18.8	17.1
R_{free}(%)§	22.1	21.4
Average B-value (Å^2)	37.7	26.7
Peptide average B-value (Å^2)	46.4	29.4
Wilson B-value (Å^2)	28.8	21.0
Protein atoms	3,446	3,424
Peptide atoms	98	112
Waters	412	326
Other atoms	58	2
rmsd from ideal geometry		
Bond length (Å)	0.007	0.007
Bond angles (°)	1.07	1.21
Ramachandran statistics (%)¶		
Most favored	97.5	98.0
Allowed	2.5	2.0
Disallowed	0.0	0.0
PDB ID code	4DGY	4DGV

*Numbers in parentheses refer to the highest resolution shell.
†$R_{sym} = \Sigma_{hkl} \Sigma_i \mid I_{hkl,i} - <I_{hkl}> \mid / \Sigma_{hkl} \Sigma_i I_{hkl,I}$, where $I_{hkl,i}$ is the scaled intensity of the i^{th} measurement of relection h, k, l, $<I_{hkl}>$ is the average intensity for that reflection, and n is the redundancy.
‡$R_{cryst} = \Sigma_{hkl} \mid F_o - F_c \mid / \Sigma_{hkl} \mid F_o \mid$ x 100.
§R_{free} was calculated as for R_{cryst}, but on a test set comprising 5% of the data excluded from refinement.
¶Calculated using MOLPROBITY.

Table S2. van der Waals interactions

C2 crystal form			$P2_1$ crystal form		
Peptide residue	Fab residue	Distance (Å)	Peptide residue	Fab residue	Distance (Å)
Trp^{420} CH2*	H Trp^{47} CH2	4.2	Trp^{420} CH2*	H Trp^{47} CZ2	4.1
Leu^{413} CD2	H Val^{50} CG1	4.1	Trp^{420} CH2	H Trp^{47} CH2	3.9
Leu^{413} CB	H Trp^{52} CB	4.1	Trp^{420} CZ2	H Trp^{47} CH2	4.2
Leu^{413} CB	H Trp^{52} CG	3.4	Leu^{413} CD2	H Val^{50} CG2	4.2
Leu^{413} N	H Trp^{52} CD1	2.9	Leu^{413} CD2	H Val^{50} CG1	4.0
Leu^{413} CB	H Trp^{52} CD1	3.3	Trp^{420} CZ3	H Val^{50} CG1	4.2
Leu^{413} CA	H Trp^{52} CD1	3.6	Trp^{420} CH2	H Val^{50} CG1	4.2
Gln^{412} C	H Trp^{52} CD1	3.7	Leu^{413} CB	H Trp^{52} CB	4.0
Gln^{412} CA	H Trp^{52} CD1	3.9	Leu^{413} CB	H Trp^{52} CG	3.6
Leu^{413} CB	H Trp^{52} CD2	3.6	Leu^{413} N	H Trp^{52} CD1	3.6
Leu^{413} CD2	H Trp^{52} CD2	4.0	Leu^{413} CB	H Trp^{52} CD1	3.7
Ile^{422} CD1	H Trp^{52} NE1	3.3	Gln^{412} C	H Trp^{52} CD1	4.0
Leu^{413} CB	H Trp^{52} NE1	3.4	Leu^{413} CB	H Trp^{52} CD2	3.8
Leu^{413} CA	H Trp^{52} NE1	3.7	Leu^{413} CD2	H Trp^{52} CD2	4.1
Ile^{422} CD1	H Trp^{52} CE2	3.5	Ile^{422} CD1	H Trp^{52} CE2	3.8
Leu^{413} CB	H Trp^{52} CE2	3.6	Leu^{413} CB	H Trp^{52} CE2	4.1
Leu^{413} CD2	H Trp^{52} CE3	4.0	Leu^{413} CD2	H Trp^{52} CE3	3.8
Ile^{422} CD1	H Trp^{52} CZ2	3.2	Ile^{422} CD1	H Trp^{52} NE1	3.7
Leu^{413} CD1	H Trp^{52} CZ2	4.3	Ile^{422} CD1	H Trp^{52} CZ2	3.5
Gln^{412} CG	H Asn^{56} CG	4.1	Arg^{1} CB	H Phe^{52A} CD2	4.0
Gln^{412} CA	H Asn^{56} OD1	3.6	Arg^{1} CG	H Phe^{52A} CD2	4.1
Gln^{412} CG	H Asn^{56} OD1	3.6	Arg^{1} CD	H Phe^{52A} CE2	4.0
Gln^{412} C	H Asn^{56} OD1	3.7	Arg^{1} CG	H Phe^{52A} CE2	4.0
Leu^{413} CB	H Asn^{56} OD1	3.8	Arg^{1} CB	H Phe^{52A} CE2	4.1
Trp^{420} CH2	H Tyr^{58} CB	4.2	Leu^{413} N	H Asn^{56} CG	3.8
Trp^{420} CZ3	H Tyr^{58} CG	4.1	Gln^{412} CA	H Asn^{56} ND2	3.6
Asn^{415} CB	H Tyr^{58} CD1	4.0	Gln^{412} C	H Asn^{56} ND2	3.7
Trp^{420} CZ3	H Tyr^{58} CD2	3.7	Gln^{412} CG	H Asn^{56} ND2	3.7
Leu^{413} CD2	H Tyr^{58} CD2	4.2	Leu^{413} CB	H Asn^{56} ND2	3.7
Asn^{415} CB	H Tyr^{58} CE1	3.6	Leu^{413} CA	H Asn^{56} ND2	3.8
Leu^{413} O	H Tyr^{58} CE2	3.5	Trp^{420} CH2	H Tyr^{58} CB	4.2
Asn^{415} CB	H Tyr^{58} CE2	4.2	Trp^{420} CZ3	H Tyr^{58} CB	4.2
Asn^{415} N	H Tyr^{58} CZ	3.5	Asn^{415} CB	H Tyr^{58} CD1	3.8
Asn^{415} CB	H Tyr^{58} CZ	3.7	Trp^{420} CZ3	H Tyr^{58} CD2	4.0
Ile^{414} CA	H Tyr^{58} OH	3.3	Leu^{413} CD2	H Tyr^{58} CD2	4.2
Ile^{414} C	H Tyr^{58} OH	3.6	Asn^{415} CB	H Tyr^{58} CE1	3.6
Ile^{422} CG1	H Leu^{98} CD2	4.2	Leu^{413} O	H Tyr^{58} CE2	3.4
Leu^{413} CD1	H Phe^{100C} CD2	4.0	Asn^{415} N	H Tyr^{58} CE2	3.9
Ile^{422} CG1	H Phe^{100C} CD2	4.1	Leu^{413} C	H Tyr^{58} CE2	4.0
Ile^{422} CD1	H Phe^{100C} CD2	4.1	Asn^{415} CB	H Tyr^{58} CE2	4.1
Ile^{422} CG1	H Phe^{100C} CE2	3.7	Asn^{415} N	H Tyr^{58} CZ	3.4
Leu^{413} CD1	H Phe^{100C} CE2	3.8	Asn^{415} CB	H Tyr^{58} CZ	3.7
Ile^{422} CD1	H Phe^{100C} CE2	4.1	Ile^{414} CA	H Tyr^{58} OH	3.5
Trp^{420} CB	H Phe^{100C} CE2	4.1	Ile^{414} C	H Tyr^{58} OH	3.7
Ile^{422} CG1	H Phe^{100C} CZ	3.8	Arg^{1} NH1	H Leu^{98} CB	3.9
His^{421} CA	H Phe^{100C} CZ	4.1	Arg^{1} NH1	H Leu^{98} CD1	3.1
Trp^{420} CG	H Ile^{100D} CG1	4.0	Arg^{1} CD	H Leu^{98} CD1	3.5
Trp^{420} CB	H Ile^{100D} CG1	4.1	Arg^{1} CZ	H Leu^{98} CD1	3.8
Trp^{420} CD1	H Ile^{100D} CG2	4.3	Arg^{1} NE	H Leu^{98} CD1	4.0
Leu^{413} CD1	H Ile^{100D} CD1	4.0	Ile^{422} CG2	H Leu^{98} CD1	4.3
Leu^{413} CD2	H Ile^{100D} CD1	4.1	Ile^{422} CG1	H Leu^{98} CD2	4.0
Trp^{420} CE3	H Ile^{100D} CD1	4.3	Ile^{422} CD1	H Leu^{98} CD2	4.3
Trp^{420} CD1	L Arg^{91} C	4.1	Ile^{422} CG1	H Phe^{100C} CG	3.9
Trp^{420} CD1	L Arg^{91} O	3.0	Ile^{422} CG1	H Phe^{100C} CD2	3.7
Trp^{420} NE1	L Arg^{91} O	3.5	Ile^{422} CD1	H Phe^{100C} CD2	3.9
Trp^{420} CB	L Arg^{91} NH1	3.6	Leu^{413} CD1	H Phe^{100C} CD2	4.1
Gly^{418} O	L Ser^{92} O	3.5	Ile^{422} CG1	H Phe^{100C} CD1	4.0
Ser^{419} CA	L Ser^{92} O	3.8	Ile^{422} CG1	H Phe^{100C} CE2	3.6
Gly^{418} O	L Asn^{93} CA	3.4	Trp^{420} CB	H Phe^{100C} CE2	3.9
Gly^{418} C	L Asn^{93} CA	4.0	Trp^{420} C	H Phe^{100C} CE2	4.1
Gly^{418} O	L Asn^{93} C	3.5	Ile^{422} CD1	H Phe^{100C} CE2	4.1

Table S2. Cont.

C2 crystal form			$P2_1$ crystal form		
Peptide residue	Fab residue	Distance (Å)	Peptide residue	Fab residue	Distance (Å)
Gly^{418} CA	L Asn^{93} OD1	3.5	Leu^{413} CD1	H Phe^{100C} CE2	4.2
Gly^{418} C	L Trp^{94} N	3.5	Ile^{422} CG1	H Phe^{100C} CE1	3.8
Gly^{418} CA	L Trp^{94} N	3.7	Ile^{422} CG1	H Phe^{100C} CZ	3.6
Trp^{420} NE1	L Trp^{94} CA	3.6	Trp^{420} CG	H Ile^{100D} CG1	3.9
Gly^{418} O	L Trp^{94} CA	3.7	Trp^{420} CD2	H Ile^{100D} CG1	4.0
Trp^{420} CZ2	L Trp^{94} CA	4.1	Trp^{420} CB	H Ile^{100D} CG1	4.1
Trp^{420} NE1	L Trp^{94} C	3.6	Trp^{420} CD1	H Ile^{100D} CG2	4.2
Gly^{418} CA	L Trp^{94} CG	4.0	Leu^{413} CD1	H Ile^{100D} CD1	4.0
Gly^{418} CA	L Trp^{94} CD1	3.4	Trp^{420} CE3	H Ile^{100D} CD1	4.0
Asn^{415} ND2	L Trp^{94} CD2	3.6	Leu^{413} CD2	H Ile^{100D} CD1	4.1
Asn^{415} ND2	L Trp^{94} CE2	3.7	Trp^{420} CD2	H Ile^{100D} CD1	4.1
Gly^{418} CA	L Trp^{94} CE2	4.0	Trp^{420} CD1	L Arg^{91} C	4.0
Asn^{415} ND2	L Trp^{94} CE3	3.5	Trp^{420} CD1	L Arg^{91} O	2.9
Trp^{420} CZ2	L Trp^{94} CE3	3.7	Trp^{420} O	L Arg^{91} NH2	3.5
Trp^{420} CH2	L Trp^{94} CE3	3.9	Trp^{420} CB	L Arg^{91} NH2	3.5
Gly^{418} CA	L Trp^{94} NE1	3.4	Gly^{418} O	L Asn^{93} CA	3.6
Gly^{418} N	L Trp^{94} NE1	3.7	Gly^{418} O	L Asn^{93} C	3.6
Asn^{415} OD1	L Trp^{94} CZ2	3.5	Gly^{418} CA	L Asn^{93} OD1	3.3
Asn^{415} ND2	L Trp^{94} CZ2	3.7	Gly^{418} C	L Trp^{94} N	3.7
Asn^{415} CG	L Trp^{94} CZ2	3.8	Gly^{418} CA	L Trp^{94} N	3.9
Asn^{415} ND2	L Trp^{94} CZ3	3.5	Trp^{420} NE1	L Trp^{94} CA	3.6
Trp^{420} CH2	L Trp^{94} CZ3	3.9	Gly^{418} O	L Trp^{94} CA	3.7
Trp^{420} CZ2	L Trp^{94} CZ3	4.2	Trp^{420} CZ2	L Trp^{94} CA	4.0
Asn^{415} ND2	L Trp^{94} CH2	3.6	Trp^{420} NE1	L Trp^{94} C	3.4
Asn^{415} CG	L Trp^{94} CH2	3.8	Trp^{420} CZ2	L Trp^{94} C	4.1
Trp^{420} CZ2	L Ile^{96} CG1	3.9	Trp^{420} CE2	L Trp^{94} O	3.7
Trp^{420} CZ2	L Ile^{96} CD1	4.1	Trp^{420} CD1	L Trp^{94} O	3.7
			Gly^{418} CA	L Trp^{94} CD1	4.2
			Gly^{418} CA	L Trp^{94} CE2	4.1
			Asn^{415} ND2	L Trp^{94} CE3	3.5
			Trp^{420} CZ2	L Trp^{94} CE3	3.7
			Trp^{420} CH2	L Trp^{94} CE3	3.9
			Asn^{415} ND2	L Trp^{94} CZ3	3.4
			Asn^{415} CG	L Trp^{94} CZ3	3.9
			Trp^{420} CH2	L Trp^{94} CZ3	4.0
			Trp^{420} CZ2	L Trp^{94} CZ3	4.2
			Asn^{415} ND2	L Trp^{94} CH2	3.9
			Asn^{415} CG	L Trp^{94} CH2	4.0
			Trp^{420} CZ2	L Ile^{96} CG1	3.9
			Trp^{420} CZ2	L Ile^{96} CD1	3.9

Interactions determined by contacsym (*Materials and Methods*). Numbering for the peptide follows the E2 numbering scheme except for Arg-1, which was artificially inserted to enhance solubility. Fab numbering follows the Kabat numbering scheme.
*Atom involved in interaction.

Table S3. Hydrogen bond interactions

C2 crystal form					$P2_1$ crystal form				
Peptide residue	Atom type*	Fab residue	Atom type*	Distance (Å)	Peptide residue	Atom type*	Fab residue	Atom type*	Distance (Å)
Leu^{413}	N	$HAsn^{56}$	OD1	2.9	Leu^{413}	O	$HTyr^{58}$	OH	3.6
Leu^{413}	O	$HAsn^{56}$	ND2	3.0	Gly^{418}	O	$LTrp^{94}$	N	2.8
Leu^{413}	O	$HTyr^{58}$	OH	3.3	Trp^{420}	NE1	$LTrp^{94}$	O	2.8
Asn^{415}	N	$HTyr^{58}$	OH	3.1					
Gly^{418}	O	$LTrp^{94}$	N	2.7					
Trp^{420}	NE1	$LTrp^{94}$	O	3.0					

Hydrogen bonds determined by hbplus (*Materials and Methods*). Numbering for the peptide follows the E2 numbering scheme, and numbering for the Fab follows the Kabat scheme. The capitalized letter in front of the residue designates heavy change (H) and light chain (L).
*Atom involved in interaction.

Table S4. Amino acid sequence variation analysis of HCV E2 protein using the ViPR resource

E2 position	Consensus	Alignment details	No. of sequences
412	Gln	Gln = 2020, Arg = 39, His = 37, Asn = 17, Ser = 15, Glu = 10, Tyr = 7, Lys = 6, Met = 5, Gly = 2, Del = 2, Leu = 1	2,161
413	Leu	Leu = 2158, Del = 2, Phe = 1	2,161
414	Ile	Ile = 1460, Val = 679, Met = 10, Xaa = 5, Thr = 4, Del = 2, Asn = 1	2,161
415	Asn	Asn = 2100, Lys = 23, His = 13, Tyr = 10, Ser = 5, Asp = 3, Arg = 2, Xaa = 2, Del = 2, Glu = 1	2,161
416	Thr	Thr = 1840, Ser = 267, Ala = 27, Asn = 12, Lys = 8, Ile = 2, Arg = 2, Del = 2, Val = 1	2,161
417	Asn	Asn = 2104, Ser = 35, Asp = 10, His = 3, Glu = 2, Gly = 2, Lys = 2, Del = 2, Gln = 1	2,161
418	Gly	Gly = 2157, Asp = 2, Del = 2	2,161
419	Ser	Ser = 2152, Asn = 3, Arg = 2, Thr = 2, Del = 2	2,161
420	Trp	Trp = 2158, Arg = 1, Del = 2	2,161
421	His	His = 2158, Del = 2, Asp = 1	2,161
422	Ile	Ile = 2095, Val = 56, Leu = 8, Del = 2	2,161
423	Asn	Asn = 2159, Del = 2	2,161

Data (September 29, 2011) were obtained from the ViPR online (http://www.viprbrc.org). Del, deletion; Xaa, ambiguity residue in the translated E2 sequence.